© 2017. Published by The Company of Biologists Ltd | Journal of Cell Science (2017) 130, 1365-1378 doi:10.1242/jcs.200493

RESEARCH ARTICLE

Neuropilin 1 binds PDGF-D and is a co-receptor in PDGF-D–PDGFRβ signaling

Lars Muhl*, Erika Bergsten Folestad, Hanna Gladh, Yixin Wang, Christine Moessinger, Lars Jakobsson and Ulf Eriksson

ABSTRACT

Platelet-derived growth factor (PDGF)-D is a PDGF receptor β (PDGFRβ)-specific ligand implicated in a number of pathological conditions, such as cardiovascular disease and cancer, but its biological function remains incompletely understood. In this study, we demonstrate that PDGF-D binds directly to neuropilin 1 (NRP1), in a manner that requires the PDGF-D C-terminal Arg residue. Stimulation with PDGF-D, but not PDGF-B, induced PDGFRβ–NRP1 complex formation in fibroblasts. Additionally, PDGF-D induced translocation of NRP1 to cell–cell junctions in endothelial cells, independently of PDGFRβ, altering the availability of NRP1 for VEGF-A–VEGFR2 signaling. PDGF-D showed differential effects on pericyte behavior in *ex vivo* sprouting assays compared to PDGF-B. Furthermore, PDGF-D-induced PDGFRβ–NRP1 interaction can occur in *trans* between molecules located in different cells (endothelial cells and pericytes). In summary, we show that NRP1 can act as a co-receptor for PDGF-D–PDGFRβ signaling and is possibly implicated in intercellular communication in the vascular wall.

KEY WORDS: PDGF-D, NRP1, Co-receptor, Endothelial cells, Pericyte, Trans-signaling

INTRODUCTION

Platelet-derived growth factor (PDGF)-D is the most recently discovered member of the PDGF family of growth factors. PDGFs fulfill important functions during embryonic development as well as in adult physiology (Andrae et al., 2008; Bergsten et al., 2001; LaRochelle et al., 2001).

The PDGF family consists of four ligands, PDGF-A to -D. They are secreted as disulfide-bonded homo- or heterodimers, denoted PDGF-AA, -AB, -BB, -CC and -DD, which bind to and signal through two tyrosine kinase receptors, PDGF receptor (PDGFR)α and PDGFRβ (Fredriksson et al., 2004; Heldin and Westermark, 1999). The PDGF ligands share a conserved growth factor domain and, in addition, PDGF-A and -B also contain C-terminal retention motifs important for their physiological function (Andrae et al., 2013; Lindblom et al., 2003). PDGF-A and PDGF-B are secreted in their active form, while secreted PDGF-C and -D polypeptide chains contain a N-terminal CUB (homology to complement components C1r/C1 s, Uegf, Bmp1) domain that needs to be proteolytically removed to enable receptor binding, and are thus produced and released as latent, inactive growth factors (Bergsten et al., 2001; Li et al., 2000; Ustach and Kim, 2005). The activation of PDGF-D is executed by serine proteases, such as urokinase-type plasminogen activator (uPA, also known as PLAU) or matriptase (Ehnman et al., 2009; Ustach et al., 2010).

PDGF-D is a ligand for PDGFRβ, suggesting that it has a functional overlap with PDGF-B, which also binds to the same receptor (Andrae et al., 2008; Bergsten et al., 2001). PDGF-D and PDGFRβ are both expressed in the vasculature. PDGFRβ is persistently expressed in pericytes (Lindahl et al., 1997), while PDGF-D expression changes in a spatial and temporal manner. The main sites of PDGF-D expression appear to be arterial endothelial cells, but it can also be expressed in vascular smooth muscle cells and presumably other subpopulations of mural cells (Gladh et al., 2016). PDGF-D, in contrast to PDGF-B, is dispensable for murine embryonic development (Gladh et al., 2016), but has been shown to, for example, stimulate the proliferation of PDGFRβ-positive cells in fibrotic processes and various cancers (Andrae et al., 2008; Cortez et al., 2016; Ponten et al., 2005; Wang et al., 2010) and is associated with cardiovascular disease (Hsu and Smith, 2012). However, the biology of PDGF-D remains largely enigmatic. Therefore, it is of interest to better understand the role of PDGF-D in physiological as well as pathological conditions.

Increasing evidence shows that PDGFR signaling can be modified by neuropilin 1 (NRP1), a multifunctional trans-membrane receptor protein (Kofler and Simons, 2016). NRP1 is well described as a co-receptor for members of the class 3 semaphorins (SEMA3) or vascular endothelial growth factors (VEGFs) (Koch, 2012; Zachary, 2014). Structurally, NRP1 is comprised of seven sub-domains whereof the first five are extracellular; two CUB domains (a1 and a2), two coagulation factor V/VIII domains (FV/VIII; b1 and b2) and a meprin, A5 μ-phosphatase domain (MAM; c). NRP1 contains only a short cytosolic tail with a PDZ-binding domain lacking internal signaling activity (Pellet-Many et al., 2008). The different ligand families bind to different sites of NRP1; SEMA3A binding requires the first three sub-domains of NRP1 (a1, a2, and b1) while binding of VEGF-A requires the b1 and b2 domains (Gu et al., 2002; Mamluk et al., 2002). Despite reports of NRP1 interaction with PDGFs (Ball et al., 2010; Banerjee et al., 2006; Cao et al., 2010; Pellet-Many et al., 2011), a specific binding site for PDGFs in NRP1 is not known. In addition, interactions of NRP1 with PDGFRα or PDGFRβ have been suggested (Pellet-Many et al., 2015), but its potential role in PDGF–PDGFR signaling remains elusive.

Here we demonstrate that PDGF-D directly binds to NRP1 and induces PDGFRβ–NRP1 complex formation. These NRP1–PDGFRβ complexes can form between proteins expressed in the same cell (in *cis*) or between these proteins in two adjacent cells (in *trans*). We identified the PDGF-D C-terminal arginine residue (Arg^{370}), and the b1 and b2 domains of NRP1 to be crucial for the direct interaction of PDGF-D with NRP1. Furthermore, PDGF-D induces NRP1 translocation to endothelial cell junctions

Department of Medical Biochemistry and Biophysics, Division of Vascular Biology, Karolinska Institutet, Scheeles väg 2, A3:P4, Stockholm S-17177, Sweden.

*Author for correspondence (lars.muhl@ki.se)

L.M., 0000-0003-0952-0507; U.E., 0000-0002-4439-3980

Received 7 December 2016; Accepted 19 February 2017

Journal of Cell Science (2017) 130, 1365-1378 doi:10.1242/jcs.200493

independently of PDGFRβ, possibly changing the availability of NRP1 for other endothelial signaling pathways. With these novel insights into the co-receptor function of NRP1 for PDGF-D–PDGFRβ signaling, we reveal differential signaling between PDGF-D and PDGF-B and provide the underlying mechanism. This knowledge may contribute to a better understanding of the physiological and pathological role(s) of PDGF-D as well as NRP1.

RESULTS

The C-terminal PDGF-D sequence exhibits unique features in comparison with PDGF-B

An amino acid sequence alignment of PDGF-B and PDGF-D (core) showed the conserved cysteine-knot structure and a high overall sequence similarity (Fig. 1A). Sequence alignment of PDGF-D with the VEGF-A isoform VEGF-A_{121} and VEGF-E also showed the conserved cysteine-knot structure. Additionally, a common C-terminal arginine (Arg) residue was revealed (Fig. 1A, red box), which has previously been shown to be important for binding of specific VEGF-A isoforms and VEGF-E to NRP1 (Cebe-Suarez et al., 2008; Delcombel et al., 2013; Parker et al., 2012). This suggests a possible interaction of PDGF-D with NRP1, similar to that described for some members of the VEGF family. Importantly, PDGF-B lacks a C-terminal Arg residue, indicating a putative difference with respect to co-receptor engagement between PDGF-D and PDGF-B.

The C-terminal Arg^{370} residue of PDGF-D is required for direct binding to NRP1

To test whether the C-terminal motif of PDGF-D enables an interaction with NRP1, we performed protein-binding studies. The results showed a dose-dependent binding of PDGF-D to NRP1, while PDGF-B, the other PDGFRβ ligand, showed no binding to NRP1 (Fig. 1B). Previously, it was shown that the FV/FVIII domains (b1 and b2) of NRP1 are important for the binding of VEGF-A to NRP1 (Gu et al., 2002; Mamluk et al., 2002). To assess whether PDGF-D binds in a similar way to NRP1 as does VEGF-A, we produced domain-deleted NRP1 mutant proteins and tested their binding to PDGF-D. NRP1 proteins lacking either the b1 or b2 domain (Δb1 or Δb2, respectively) showed impaired ability to bind to PDGF-D (Fig. 1C), while Δa1+7 and Δa2 bound with an efficiency comparable to wild-type (wt) NRP1, suggesting a similar binding mode of PDGF-D and VEGF-A to NRP1 (NRP1 deletion constructs are described in Gu et al., 2002). To demonstrate the requirement of the C-terminal Arg^{370} residue in PDGF-D for NRP1 binding we produced PDGF-D mutant proteins with either the truncation of the C-terminal Arg^{370} (-R), or the exchange of the C-terminal Arg^{370} for a glycine residue (R→G) and compared those to wt PDGF-D (Fig. S1A). Overexpression of the recombinant PDGF-D proteins in PDGFRβ overexpressing porcine aortic endothelial (PAE-Rβ) cells resulted in similar phosphorylation of PDGFRβ, demonstrating comparable binding and activation characteristics to PDGFRβ among the different mutant and wt PDGF-D proteins (Fig. S1B). To test the binding abilities of the mutant proteins to NRP1, we performed a ligand blot assay with recombinant NRP1 and concentrated supernatant from COS-1 cells overexpressing mutant PDGF-D proteins. Only recombinant PDGF-D with the wt C-terminal sequence exhibited binding to NRP1 (Fig. 1D), while removal of the C-terminal Arg^{370} (-R), or the exchange to Gly (R→G), resulted in the inability to bind NRP1. This confirmed that the C-terminal Arg^{370} residue is required for binding of PDGF-D to NRP1 and distinguishes between the co-receptor-binding characteristics of PDGF-D and PDGF-B.

Heparin binds to PDGF-D and promotes the interaction of PDGF-D with NRP1

The common sequence features hint at a similar binding mechanism for PDGF-D and VEGF-A to NRP1. As heparan sulfate proteoglycans (HSPG) or heparin can function as co-factors for VEGF-A–NRP1 interaction (Mamluk et al., 2002), we compared PDGF-D to VEGF-A isoforms that exhibit different binding characteristics to NRP1 and HSPG. We confirmed that heparin promoted the interaction of the VEGF-A isoforms VEGF-A_{165} and VEGF-A_{189} with NRP1 (Fig. 1E). Interestingly, the addition of heparin augmented the binding of NRP1 to PDGF-D core protein (the activated form), but not to full-length (FL-)PDGF-D (Fig. 1E). Heparin did not induce a binding of PDGF-B to NRP1 (Fig. 1E). These results suggest that PDGF-D, upon activation by removal of the CUB domain, can bind to heparin, which we could confirm by a direct binding assay of biotin-labeled heparin to immobilized PDGF-D (core and FL) and other growth factors (Fig. 1F). The PDGF-D core protein bound heparin, while FL-PDGF-D showed only weak binding to heparin, VEGF-A_{121} failed to bind heparin and, as expected, VEGF-A_{189} bound especially strong to heparin (Fig. 1F). PDGF-B proteins failed to bind heparin (Fig. 1F). The observation that only active PDGF-D could bind heparin led us to the hypothesis that cleavage of PDGF-D exposes its heparin-binding motif. Sequence analysis revealed an enrichment of positive charged amino acids (Arg or Lys) within the N-terminal sequence of active PDGF-D as a possible heparin-binding motif, located downstream (C-terminal) of the activating cleavage site (Ustach and Kim, 2005) (Fig. S1D). Modeling of the three-dimensional structure of core PDGF-D supported the hypothesis for a heparin-binding motif located between the activating cleavage site and the first cysteine in the cysteine-knot structure (Fig. S1D).

PDGF-D induces the interaction of PDGFRβ and NRP1

To investigate whether NRP1 might have relevance for the PDGF-D–PDGFRβ signaling cascade, we stimulated fibroblasts (BJ-hTERT) with PDGF-D or PDGF-B (Fig. 2). Immunofluorescence analysis of stimulated BJ-hTERT cells showed strong PDGFRβ clustering and internalization in response to both growth factors (Fig. 2Ab″,c″). However, only PDGF-D promoted the colocalization of PDGFRβ and NRP1 and concomitant clustering and internalization of NRP1 (Fig. 2Ab′-b′″). Quantification followed by Pearson's correlation showed that PDGF-D, but not PDGF-B, induced colocalization of PDGFRβ and NRP1, while both PDGF-D and PDGF-B caused co-clustering of PDGFRβ and EEA1 (early endosome antigen 1) (Fig. 2B), highlighting equally efficient activation and internalization of PDGFRβ in response to PDGF-D and PDGF-B.

Co-immunoprecipitation experiments further confirmed a PDGF-D-dependent interaction of PDGFRβ with NRP1 (Fig. 2C). BJ-hTERT cells stimulation with PDGF-D or PDGF-B followed by a NRP1 pull-down showed that PDGFRβ co-precipitated with NRP1 upon stimulation with PDGF-D, but not with PDGF-B. Both growth factors efficiently stimulated PDGFRβ-phosphorylation, as seen in the input samples, demonstrating no obvious difference between PDGF-D and PDGF-B with respect to PDGFRβ binding and activation (Fig. 2C). Nevertheless, in response to PDGF-D stimulation, NRP1 co-immunoprecipitated PDGFRβ was also phosphorylated, demonstrating that the NRP1-associated PDGFRβ is activated (Fig. 2D). This suggests that NRP1 can participate in active PDGF-D–PDGFRβ signaling.

Stimulation of BJ-hTERT cells followed by analysis of whole-cell lysates revealed that only PDGF-D-dependent internalization of NRP1 together with PDGFRβ results in degradation of NRP1 (Fig. 3), while both PDGF-D and PDGF-B induce degradation of

Journal of Cell Science (2017) 130, 1365-1378 doi:10.1242/jcs.200493

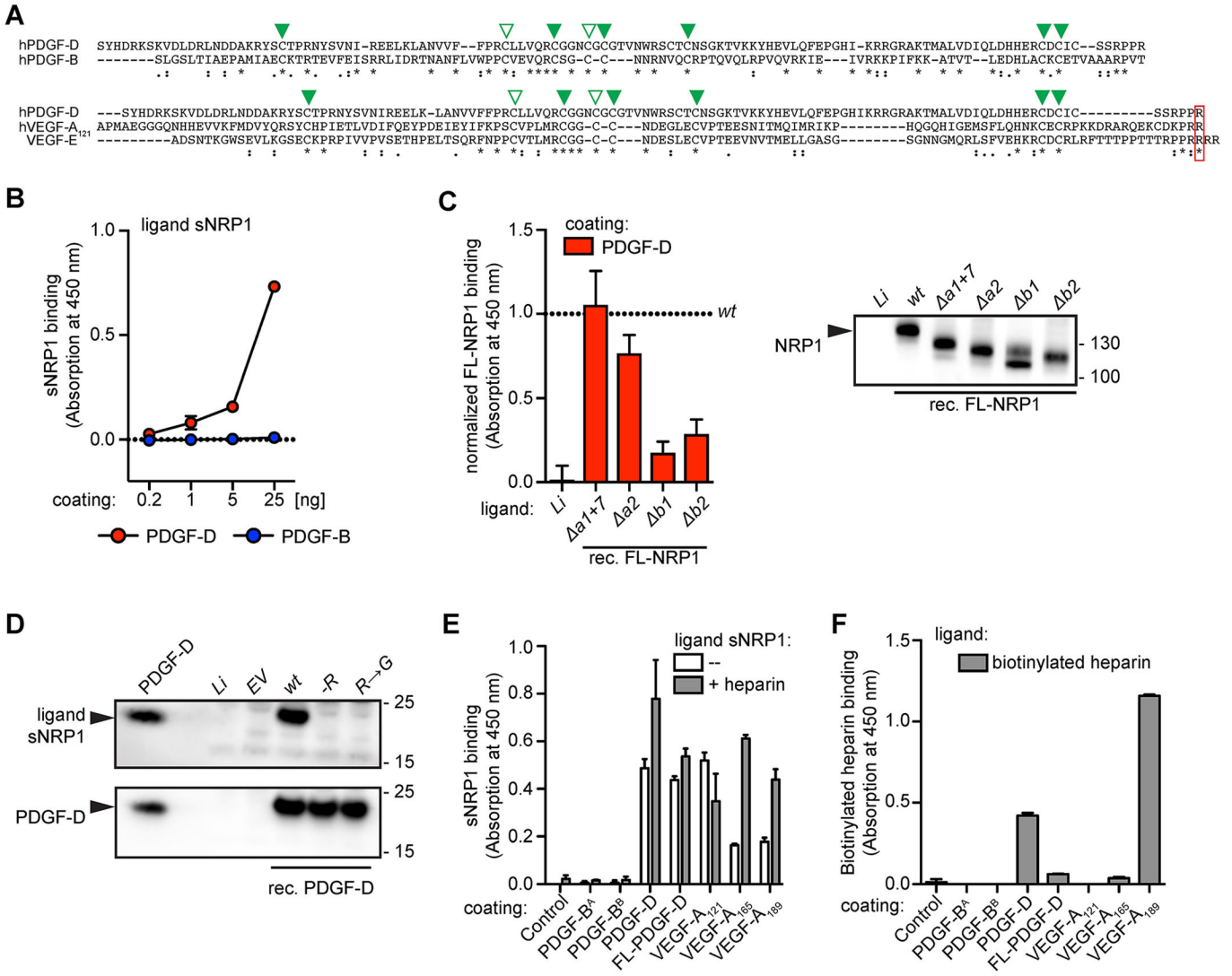

Fig. 1. PDGF-D binds to NRP1 via its C-terminal Arg^{370} residue. (A) PDGF-D amino acid sequence analysis and comparison to members of the PDGF/VEGF family using the CLUSTAL online tool (., :, *, increasing grades of similarity). The upper panel shows the amino acid sequence alignment of PDGF-B and PDGF-D (core) highlighting the conserved cysteine residues (green arrowheads; open, inter-chain, closed, intra-chain). The lower panel shows the amino acid sequence alignment of PDGF-D and VEGF-A$_{121}$ and VEGF-E, showing the conserved cysteine-knot structure (green arrowheads; open, inter-chain, closed, intra-chain) and the shared C-terminal Arg residue (R, red box). (B) Soluble NRP1 (sNRP1, 0.5 µg/ml) binding to immobilized PDGF-D or PDGF-B (both 0.2–25 ng). One representative experiment is shown, samples were prepared as *n*=3 and presented as mean±s.d. (C) Cell lysates containing recombinant full-length NRP1 (rec. FL-NRP1) wt or mutant proteins (*Δa1+7*, *Δa2*, *Δb1* or *Δb2*), or cell lysates from lipofectamine-only (Li) treated cells were applied to immobilized PDGF-D (25 ng) to measure NRP1 binding. Mean±s.d. of *n*=3 independent experiments is shown, normalized to binding of wt FL-NRP1. The comparable amount of input FL-NRP1 proteins was controlled by western blotting (right). (D) Ligand blot and detection of sNRP1 binding to recombinant PDGF-D mutant proteins or commercial PDGF-D (100 ng). Concentrated supernatant containing PDGF-D mutant proteins (wt, -R or R→G) was separated by SDS-PAGE, and NRP1 binding was detected (upper panel). The total amount of recombinant PDGF-D proteins was visualized by subsequent incubation of the same membrane with anti-PDGF-D specific antibody (lower panel). (E) Protein binding assay of sNRP1 (0.5 µg/ml) without (white columns) or with heparin (10 µg/ml, gray columns) to immobilized growth factors (all coated at an amount of 25 ng). One representative experiment is shown, samples were prepared as *n*=3 and presented as mean±s.d. (F) Binding of biotinylated heparin (0.5 µg/ml) to immobilized growth factors (25 ng). One representative experiment is shown; samples were prepared as *n*=3 and presented as mean±s.d.

PDGFRβ and activate downstream signaling via AKT1 (also known as PKB), and ERK-1 and ERK-2 (ERK-1/2, also known a MAPK3 and MAPK1, respectively). Despite the engagement of NRP1 by PDGF-D, no difference in the signaling characteristics between PDGF-D and PDGF-B could be observed (Fig. 3), which is in accordance with previous reports (Borkham-Kamphorst et al., 2015).

Direct binding of PDGF-D to NRP1 is required for PDGFRβ–NRP1 colocalization

In order to test whether the C-terminal Arg^{370} of PDGF-D is required for the PDGF-D-induced colocalization of PDGFRβ and NRP1, we used proteins with mutated C-terminal Arg^{370} residues. Stimulation of BJ-hTERT cells with conditioned medium from COS-1 cells overexpressing wt PDGF-D efficiently induced PDGFRβ–NRP1 co-clustering, compared to conditioned medium from COS-1 cells transfected with the empty vector (Fig. 4Aa,b). In contrast, conditioned medium from COS-1 cells expressing PDGF-D proteins with either a truncated C-terminus, without the C-terminal Arg^{370} residue (-R) (Fig. 4Ac) or with an exchange of the C-terminal Arg^{370} residue to Gly (R→G) (Fig. 4Ad) did not induce PDGFRβ–NRP1 colocalization. Nevertheless, these mutant PDGF-D proteins could efficiently activate PDGFRβ, as indicated

Journal of Cell Science (2017) 130, 1365-1378 doi:10.1242/jcs.200493

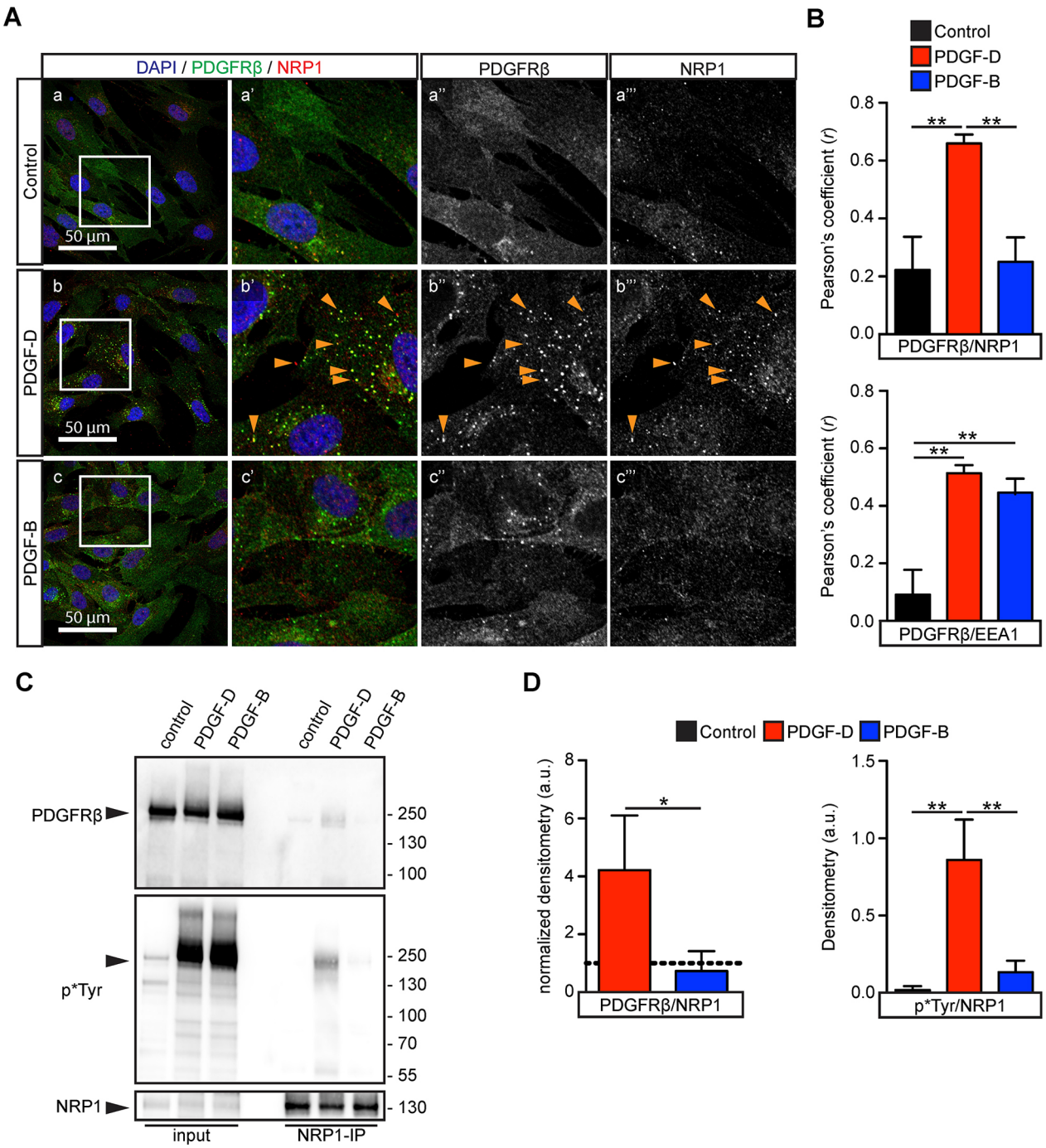

Fig. 2. PDGF-D induces the interaction of PDGFRβ and NRP1 in fibroblasts. BJ-hTERT cells were stimulated with PDGF-D or PDGF-B. (A) Non-stimulated control (a–a‴), or PDGF-D- (b–b‴) or PDGF-B- (c–c‴) (both 20 ng/ml) treated (20 min) BJ-hTERT cells, were stained with antibodies for PDGFRβ (green) and NRP1 (red). Orange arrowheads highlight subcellular clusters of NRP1. Representative images from one out of at least three independent experiments are presented. Boxed areas are shown at higher magnification on the right. (B) Quantification of PDGFRβ–NRP1 (upper panel) or PDGFRβ–EEA1 (lower panel) colocalization using the Fiji colocalization application. The mean±s.d. of *n*=3 independent experiments is shown. ***P*<0.01 (one-way ANOVA with Bonferroni post-hoc test for multiple comparisons). (C) BJ-hTERT cells were stimulated with PDGF-D or PDGF-B (both 25 ng/ml) followed by immunoprecipitation for NRP1 (C19, NRP1-IP). Input and pulldown samples were analyzed by western blotting for PDGFRβ (upper panel), phosphorylated tyrosine (p*Tyr, middle panel) and NRP1 (lower panel), all successively detected on the same membrane. One representative out of *n*=3 independent experiments is shown. (D) Quantification of densitometry measurement of western blots from the NRP1 immunoprecipitation samples.The PDGFRβ:NRP1 ratio normalized to non-stimulated control (left panel) and p*Tyr:NRP1 ratio (right panel) of *n*=3 independent experiments are presented as mean±s.d. **P*<0.05; ***P*<0.01 (unpaired, two-tailed Students' *t*-test, left panel; one-way ANOVA with Bonferroni post-hoc test for multiple comparisons, right panel).

by perinuclear PDGFRβ accumulation (Fig. 4Ab–d). In line with these observations, we could show by separate siRNA-mediated knockdown experiments of either *PDGFRB* or *NRP1* in BJ-hTERT cells, that PDGFRβ is required for PDGF-D-induced NRP1 clustering, internalization and degradation, while NRP1 is dispensable for efficient PDGFRβ activation, internalization and

Journal of Cell Science (2017) 130, 1365-1378 doi:10.1242/jcs.200493

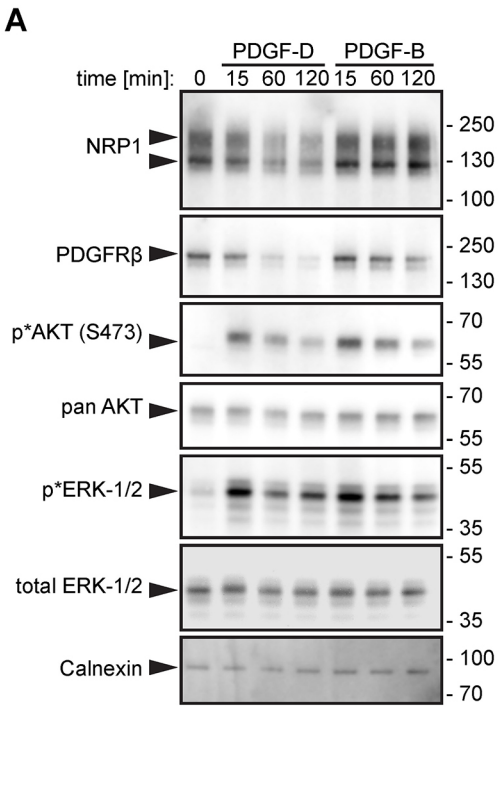

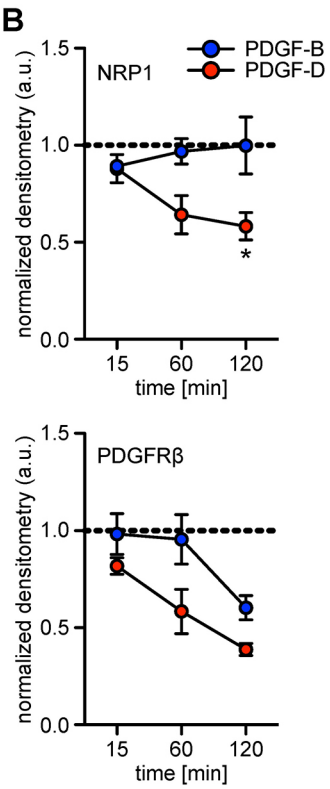

Fig. 3. PDGF-D stimulation results in degradation of NRP1 and PDGFRβ. BJ-hTERT cells were stimulated with PDGF-D or PDGF-B (10 ng/ml) for 15–120 min. (A) Representative western blots from one out of three independent direct stimulation experiments for NRP1 and PDGFRβ, downstream signaling kinases ERK-1/2 and AKT, as well as calnexin as a loading control. All proteins were successively detected on the same membrane. (B) Densitometry quantification of NRP1 (upper panel) or PDGFRβ (lower panel) protein content over time after PDGF-D or PDGF-B stimulation for n=3 independent experiments, normalized to time=0 and presented as mean±s.d. *P<0.05 (two-way ANOVA with Bonferroni post-hoc test for multiple comparisons).

degradation (Fig. S2). This is different to the reported impact of NRP1 on the VEGF-A–VEGFR2 signaling cascade (Koch, 2012; Plein et al., 2014).

PDGF-D-dependent NRP1 translocation can change VEGF-A-induced VEGFR2–NRP1 interaction in endothelial cells

Based on the well-established function of NRP1 in regulation of VEGF-A–VEGFR2 signaling, we investigated whether the interaction of PDGF-D with NRP1 could affect VEGF-A–VEGFR2–NRP1 signaling mechanisms. Stimulation of endothelial cells [human umbilical vein endothelial cells (HUVECs); high NRP1 expression and PDGFRβ negative] with VEGF-A induced co-clustering of VEGFR2 with NRP1 (Fig. 5A,B). The receptor co-clustering was effectively prevented by pre-treatment of HUVECs with PDGF-D (Fig. 5Ac,B), but not PDGF-B (Fig. 5Ad,B). Interestingly, PDGF-D treatment of HUVECs resulted in NRP1 translocation to endothelial cell junctions, indicated by colocalization of NRP1 with the tight junction protein zona occludens 1 (ZO1, also known as TJP-1) (Fig. S3A) or the gap junction protein connexin 43 (CX43, also known as GJA1) (Fig. S3B). PDGF-D stimulation rendered translocation of NRP1 exclusively to endothelial cell–cell junctions, while VEGF-A mainly induced NRP1 internalization, as seen by colocalization with EEA1-positive endosomes, presumably in complex with VEGFR2 (Fig. S3C). These observations raise the possibility that PDGF-D directly modulates the cellular localization of NRP1 in endothelial cells independently of PDGFRβ. Indeed, stimulation of HUVEC with PDGF-D followed by NRP1 immunoprecipitation revealed that PDGF-D could disrupt the VEGFR2–NRP1 complexes that were apparently present under basal cell culture conditions (Fig. 5C,D). This data suggests that PDGF-D can function as a modulator of VEGF-A–VEGFR2 signaling by influencing NRP1 distribution and availability.

Stimulation with PDGF-D retains pericyte–endothelial interaction during angiogenic sprouting to a higher extent than does PDGF-B

To implement our observation that PDGF-D binds NRP1 and thereby possibly influences PDGFRβ as well as VEGFR2 signaling pathways, we compared the effect of PDGF-D versus PDGF-B in three-dimensional *ex vivo* models of sprouting angiogenesis, mediating analysis of pericyte and endothelial cell behavior. Embryo explants or aortic ring cultures from mice with endothelial cell- and pericyte-specific endogenous fluorescence (GFP–GPI and NG2DsRed, respectively), allowing for simultaneous imaging of endothelial cells and pericytes, were investigated (Fig. 6). In embryo explant cultures, PDGF-D and PDGF-B increased the sprouting speed in a comparable manner (Fig. 6A,B). Both PDGF-D and PDGF-B, led to detachment of pericytes from the endothelial sprouts. However, PDGF-D also mediated a relative increase in pericyte coverage, which was not observed with PDGF-B (Fig. 6B). This data was confirmed in aortic ring cultures, obtaining a similar outcome (Fig. 6C). More in-depth analysis of pericyte behavior revealed that the migration speed of individual pericytes was increased in response to stimulation with PDGF-D, as well as PDGF-B, suggesting a similar magnitude of cellular activation. However, when separately analyzing either pericytes that were in contact with the endothelial sprout or those that had no contact with endothelial cells, the migration speed differed significantly in case of PDGF-D stimulation, but not when stimulated with PDGF-B (Fig. 6C). The data may suggest that PDGF-D–PDGFRβ signal transduction governed by complex formation with NRP1 in *trans*, might contribute to intercellular communication between endothelial cells and pericytes that in turn results in differential signaling outcomes from PDGF-D- or PDGF-B-induced PDGFRβ activation.

Journal of Cell Science (2017) 130, 1365-1378 doi:10.1242/jcs.200493

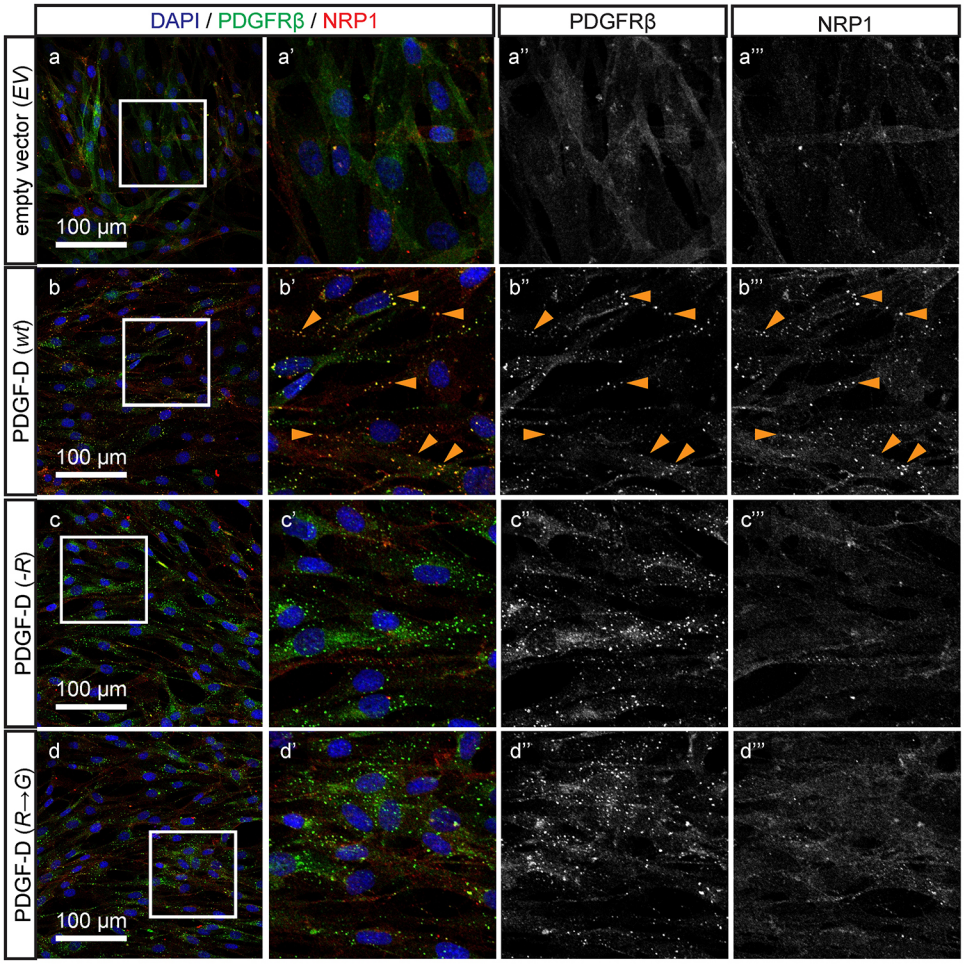

Fig. 4. PDGF-D-induced PDGFRβ–NRP1 interaction is dependent on the PDGF-D C-terminal Arg^{370}. BJ-hTERT cells were treated with conditioned medium from COS-1 cells overexpressing recombinant PDGF-D mutant proteins for 20 min. (A) Representative images of empty vector (EV) control (a–a′″), and BJ-hTERT cells treated with wt PDGF-D (b–b′″), -R PDGF-D (c–c′″) or R→G PDGF-D cells stained with antibodies for PDGFRβ (green) and NRP1 (red). Orange arrowheads highlight subcellular clusters of PDGFRβ colocalizing with NRP1. Boxed areas are shown at higher magnification on the right.

PDGF-D induces the interaction of PDGFRβ and NRP1 in *trans* between pericytes and endothelial cells

The data from the *ex vivo* experiments showed a differential effect of PDGF-D stimulation on pericyte behavior depending on their contact with endothelial cells. To evaluate the possibility that PDGF-D would induce PDGFRβ–NRP1 interaction between pericytes and endothelial cells (in *trans*) we applied *in vitro* co-culture models, where we stimulated PAE-Rβ and HUVEC, or human micro-vascular pericyte (HBVP) and HUVEC co-cultures with PDGF-D or PDGF-B. In this experimental set-up HUVECs served as the source of NRP1, while PAE-Rβ or HBVPs were the source for PDGFRβ. PAE-Rβ and HUVEC co-culture stimulation with PDGF-D, or PDGF-B, followed by NRP1 immunoprecipitation revealed the potential of PDGF-D to also induce clustering of PDGFRβ together with NRP1 in *trans* (Fig. 7A). Similar to the BJ-hTERT cell experiments, PDGF-D promoted the co-immunoprecipitation of PDGFRβ with NRP1, and activation of PDGFRβ. In contrast, PDGF-B stimulation efficiently induced the phosphorylation of PDGFRβ, but did not induce the association of PDGFRβ with NRP1 (Fig. 7A). Importantly, only in the co-culture of PAE-Rβ cells together with HUVECs was a co-immunoprecipitation of PDGFRβ with NRP1 observed, highlighting the *trans*-interaction of PAE-Rβ PDGFRβ with HUVEC NRP1. Likewise, staining of HBVP–HUVEC co-cultures for PDGFRβ and NRP1 showed PDGFRβ–NRP1 co-clustering in response to PDGF-D stimulation, which appeared to be especially pronounced in HBVP protrusions in contact with HUVECs (Fig. 7B,C). Stimulation with PDGF-B did not induce PDGFRβ–NRP1 colocalization in HBVP–HUVEC co-cultures (Fig. S4A). Additionally, the NRP1 translocation to cell–cell junctions between endothelial cells could also be seen in the PDGF-D-stimulated HBVP–HUVEC co-culture (Fig. S4Ae). As expected, PDGF-D only induced downstream signaling in PDGFRβ-positive HBVPs (alone or in co-culture with HUVECs) but not in HUVEC monocultures (Fig. S4B). This suggests an exclusive PDGF-D-specific communication route between endothelial cells and pericytes mediated by the combined interaction of PDGF-D with PDGFRβ and NRP1.

DISCUSSION

Most studies on PDGF-D do not compare PDGF-D and PDGF-B biology, or when compared, both growth factors display rather identical signaling outcomes (Borkham-Kamphorst et al., 2015), leaving PDGF-D-specific functions undiscovered. This prompted us to search for features that would differentiate PDGF-D from PDGF-B.

Here, we show that PDGF-D binds to NRP1 and delineate the structural basis underlying this interaction. A required attribute found in PDGF-D, but not present in PDGF-B, is the C-terminus with the Arg^{370} residue, which is similarly seen in NRP1-binding VEGF-A isoforms. We further demonstrate that PDGF-D binding to NRP1 resembles that of VEGF-A. As for VEGF-A$_{165}$ (Gu et al., 2002; Mamluk et al., 2002), the b1 and b2 domains of NRP1 appear to be important for the interaction of PDGF-D with NRP1. Parker et al. (2012) characterized the binding pocket of NRP1 for the

Journal of Cell Science (2017) 130, 1365-1378 doi:10.1242/jcs.200493

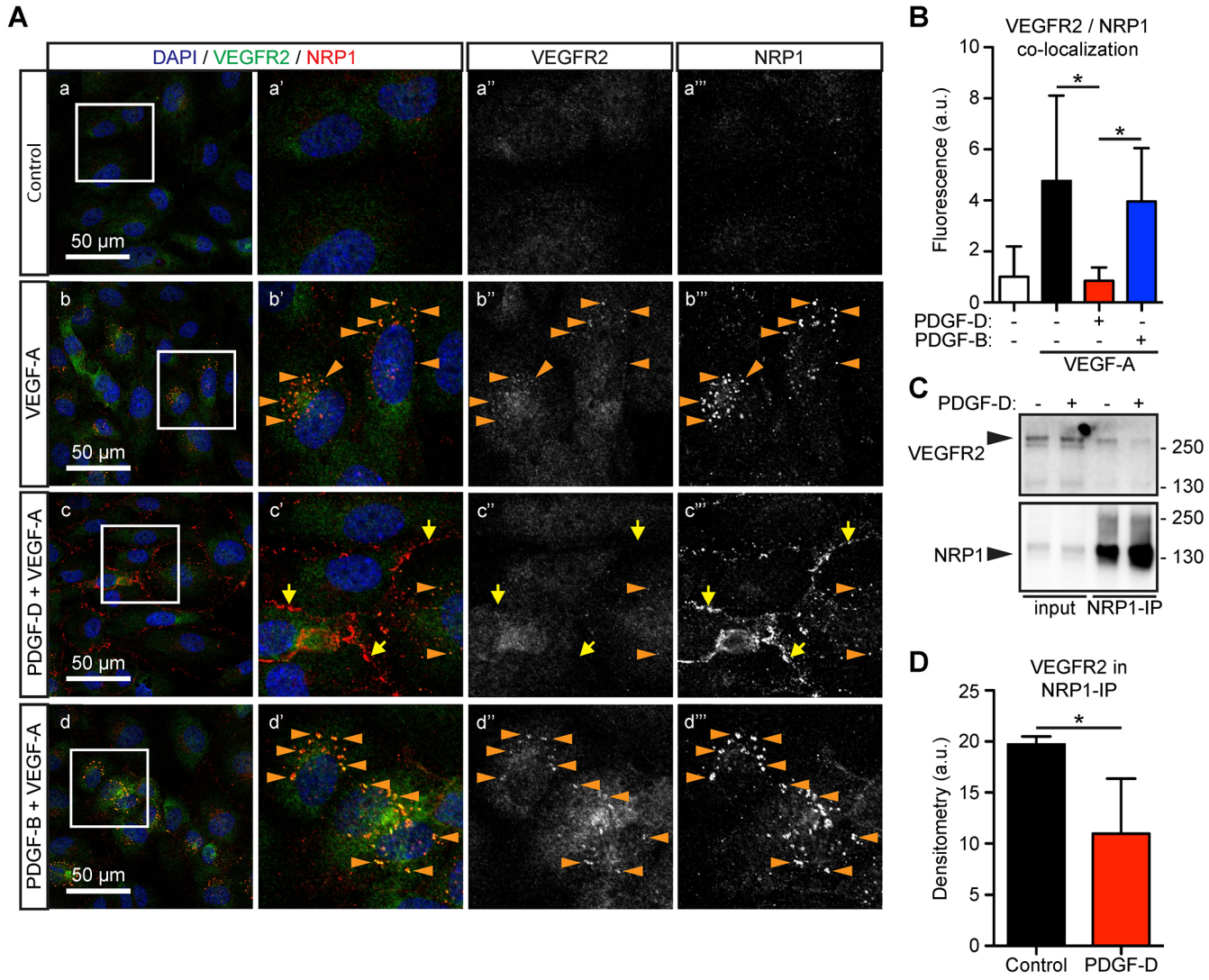

Fig. 5. PDGF-D pre-treatment impairs VEGF-A-induced VEGFR2/NRP1 colocalization. (A) HUVEC monocultures were stimulated for 20 min with VEGF-A (25 ng/ml) without pre-treatment (b) or after 20 min pre-treatment with PDGF-D (c) or PDGF-B (d) (both 20 ng/ml), and stained with antibodies for VEGFR2 (green) and NRP1 (red). Orange arrowheads highlight perinuclear VEGFR2–NRP1 colocalization. Yellow arrows in c–c‴ highlight cell–cell junction-localized NRP1. Boxed areas are shown at higher magnification on the right. (B) Quantification of VEGFR2–NRP1 colocalization in response to VEGF-A stimulation without or with pre-treatment with PDGF-D or PDGF-B. Mean±s.d. of n=3 independent experiments is shown. *P<0.05 (one-way ANOVA with Bonferroni post-hoc test for multiple comparisons). (C) HUVEC monocultures were stimulated with PDGF-D (25 ng/ml) followed by immunoprecipitation for NRP1 (C19, NRP1-IP). Input and pulldown samples were analyzed by western blotting for VEGFR2 (upper panel) and NRP1 (lower panel), successively detected on the same membrane. One representative out of three independent experiments is shown. (D) Densitometry quantification of n=3 independent experiments of VEGFR2 co-immunoprecipitation with NRP1 (ratio VEGFR2:NRP1) in response to PDGF-D stimulation, shown as mean±s.d. *P<0.05 (unpaired, two-tailed Student's t-test).

C-terminus of exon 8a-containing VEGF-A isoforms, which is located within the NRP1-b1 subdomain, and subsequent animal studies employing NRP1 mutations could confirm the lack of VEGF-A–NRP1 interaction when a single amino acid of this binding pocket was mutated (Fantin et al., 2014; Gelfand et al., 2014). We suggest that PDGF-D binds directly to NRP1, employing the same binding pocket as VEGF-A (containing the exon 8a-encoded C-terminus) and this interaction together with the NRP1-b2 domain confers correct binding of PDGF-D to NRP1 (Delcombel et al., 2013; Parker et al., 2012).

Others have reported that NRP1 can modulate PDGF-A- and PDGF-B-induced receptor signaling (Ball et al., 2010; Pellet-Many et al., 2011). However, whether these effects of NRP1 are direct or indirect remain open questions. Post-translational modification of NRP1 with chondroitin sulfate has been described to be an important aspect of NRP1-dependent modulation of PDGF-A- and PDGF-B-induced downstream signaling (Pellet-Many et al., 2011). For the protein-binding studies, we used non-modified recombinant NRP1 and thus can conclude that post-translational modification of NRP1 is not important for the interaction of PDGF-D with NRP1, although this could explain why we did not observe an interaction of PDGF-B with NRP1, as was suggested by earlier studies.

Matrix retention has previously been shown for activated (core) PDGF-D, while unprocessed FL-PDGF-D remains freely diffusible (Ehnman et al., 2009; Huang and Kim, 2015). Accordingly, we show that heparin only promotes the binding of active, core PDGF-D to NRP1, but not that of FL-PDGF-D. Likely, the heparin-binding domain is covered by the CUB domain and thus inaccessible in FL-PDGF-D. We suggest that the heparin-binding domain in PDGF-D is located between the CUB domain and the growth factor domain.

Journal of Cell Science (2017) 130, 1365-1378 doi:10.1242/jcs.200493

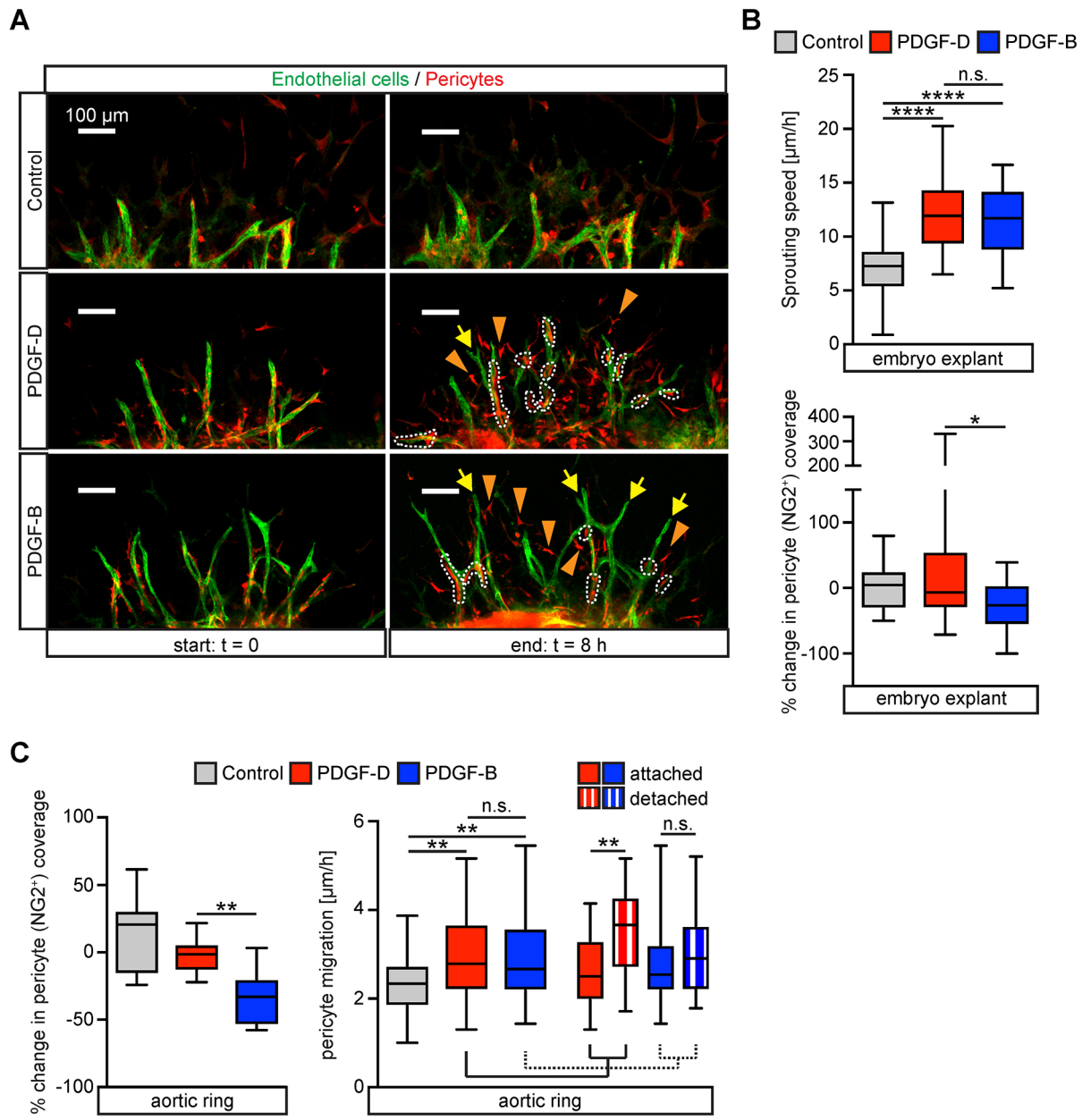

Fig. 6. PDGF-D treatment in *ex vivo* angiogenic sprouting models induces differential mural cell behavior compared to treatment with PDGF-B. *Ex vivo* cultured embryo explants (E13.5) or aortic rings (4–6-week-old mice) from GFP–GPI/NG2DsRed mice were stimulated with PDGF-D or PDGF-B (both 30 ng/ml) and monitored by time-lapse microscopy for 8 h. (A) Representative images of embryo explant cultures treated with PDGF-D or PDGF-B at the start and endpoint (8 h). Fluorescent reporter gene expression enables monitoring of endothelial cells (green) and NG^{2+} pericytes (red). Orange arrowheads highlight detached pericytes, yellow arrows indicate endothelial sprouts with low pericyte coverage and white lines highlight pericytes attached to endothelial sprouts. Scale bars: 100 µm. (B) Quantification of cellular motility by time-lapse cell tracking for overall sprouting speed (upper panel – control, *n*=33; PDGF-D; *n*=40; PDGF-B, *n*=20) or change in pericyte coverage of endothelial sprouts (lower panel – control, *n*=26; PDGF-D *n*=35; PDGF-B, *n*=17). Data is shown as box plots (the box represents the 25–75th percentiles, and the median is indicated; the whiskers show the range). **P*<0.05; *****P*<0.0001; n.s., not significant (one-way ANOVA with Bonferroni post-hoc test for multiple comparisons). (C) Quantification of cellular motility by time-lapse cell tracking for change in pericyte coverage of endothelial sprouts (left panel – control, *n*=9; PDGF-D, *n*=10; PDGF-B, *n*=9). The right panel shows individual migration speed of pericytes (control, *n*=34; PDGF-D, *n*=64; PDGF-B, *n*=43) as well as the same dataset separated for attached or detached pericytes (white striped box-plots in right panel – PDGF-D, *n*=43 and 21; PDGF-B, *n*=15 and 28). The data is presented as box-plots (the box represents the 25–75th percentiles, and the median is indicated; the whiskers show the range). ***P*<0.01; n.s., not significant (one-way ANOVA with Bonferroni post-hoc test for multiple comparisons).

Hence, proteolytic cleavage of FL-PDGF-D does not only enable PDGFRβ engagement, but potentially also determines spatial deposition of PDGF-D within the extracellular matrix. Because FL-PDGF-D is able to bind to NRP1, a cell surface retention by this interaction is possible and a contribution of NRP1 to the proteolytic processing of FL-PDGF-D awaits investigation.

Interestingly, in endothelial cells that express NRP1 but not PDGFRs, PDGF-D stimulation induces a robust translocation of NRP1 to cell–cell junctions. Thereby, PDGF-D has the potential to sequester NRP1 away from the available pool for other signaling pathways, such as VEGF-A–VEGFR2 (Koch, 2012), or transforming growth factor (TGF)-β to activin A receptor type II like 1 or TGF-β

Journal of Cell Science (2017) 130, 1365-1378 doi:10.1242/jcs.200493

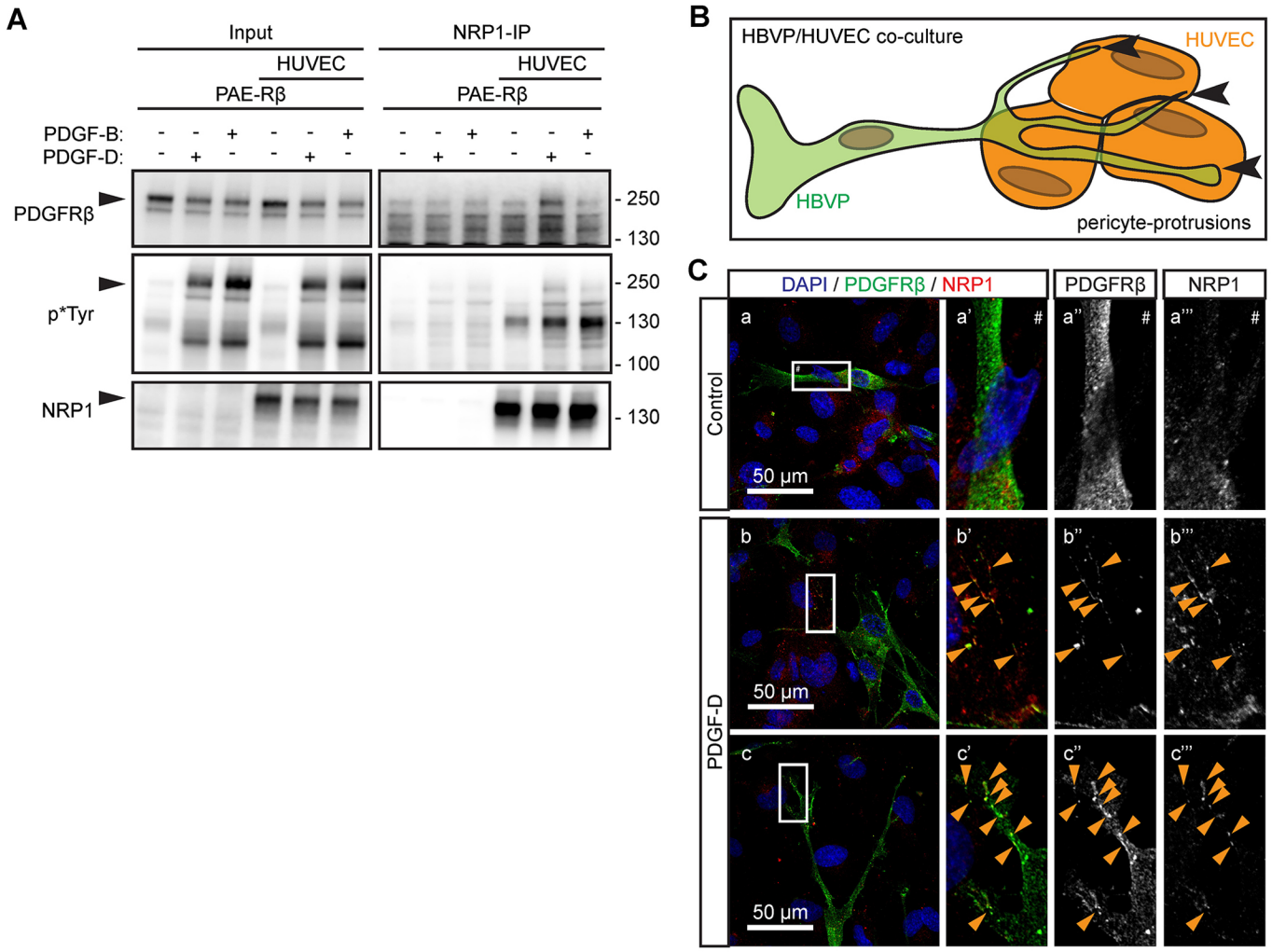

Fig. 7. PDGF-D induces the interaction of PDGFRβ and NRP1 in *trans*. (A) PAE-Rβ cells alone, or in co-culture with HUVEC, were stimulated with PDGF-D or PDGF-B (both 25 ng/ml), followed by immunoprecipitation for NRP1 (C19, NRP1-IP). Input and pulldown samples were analyzed by western blotting for PDGFRβ (upper panel), phosphorylated tyrosine (p*Tyr, middle panel), and NRP1 (lower panel), all successively detected on the same membrane. Input and NRP-IP pulldown samples were blotted onto the same membrane. Owing to the use of different exposure times, for appropriate visualization, the blots are presented as separate panels. One representative out of three independent experiments is shown. (B) Schematic illustration of the co-culture of PDGFRβ-expressing HBVPs and NRP1-expressing HUVECs, highlighting pericyte protrusions expanding over endothelial cell bodies (black arrowheads). (C) HBVPs and HUVECs in co-culture were stimulated for 15 min with 5 ng/ml PDGF-D and stained with antibodies for PDGFRβ (green) and NRP1 (red) (b–c). Orange arrowheads (b′–b‴, c′–c‴) highlight PDGFRβ–NRP1 colocalization, especially pronounced in pericyte protrusions. Boxed areas are shown in higher magnification on the right. # indicates orientation of respective high-magnification image.

receptor I (Aspalter et al., 2015; Kofler and Simons, 2016), suggesting a possible regulatory role of PDGF-D that would be dependent on availability as well as concentration of the competing NRP1 ligands. The localization of NRP1 at endothelial cell–cell junctions was recently described to induce endothelial cell permeability in a VEGFR2-independent fashion (Roth et al., 2016). The precise mechanism for this VEGFR2-independent function of NRP1 is still incompletely understood, and whether the PDGF-D-induced translocation of NRP1 is associated with increased permeability remains to be investigated. Our observation that in fibroblasts devoid of PDGFRβ, NRP1 did not translocate to cell–cell contacts suggests another yet undefined endothelial factor that promotes NRP1 trafficking and cell junction localization after PDGF-D binding.

NRP1 recruitment to VEGFR2 signaling complexes modulates intracellular sorting and trafficking of VEGFR2, thereby altering the signaling outcome of VEGF-A–VEGFR2 complexes (Ballmer-Hofer et al., 2011; Lanahan et al., 2010). Similar mechanisms have been described for PDGFRβ (Hellberg et al., 2009; Karlsson et al., 2006), and NRP1, as well as NRP2, has been suggested to be involved in PDGFR downstream signal conduction (Pellet-Many et al., 2015). Our initial analysis did, however, not reveal changes in PDGF-D–PDGFRβ downstream signaling dependent on the presence or absence of NRP1. This is not surprising since clear differences between PDGF-D- and PDGF-B-induced PDGFRβ downstream signaling have not been described (Borkham-Kamphorst et al., 2015). This might be different when PDGFRβ and NRP1 interact in *trans*, between two adjacent cells or even two different cell types. In the *trans* situation, physical hindrance would prevent internalization of both PDGFRβ and NRP1 and would lock them at the cell surface, possibly changing signaling kinetics from fast and transient to slow and persistent, as was recently shown for VEGFR2 signaling when NRP1 is presented in *trans* (Koch et al., 2014). Such a scenario would result in a spatially restricted change of PDGFRβ downstream signaling in a PDGF-D-specific manner.

Pdgfd is expressed during murine embryonic development and into adulthood. It has a mainly arterial vascular expression pattern

Journal of Cell Science (2017) 130, 1365-1378 doi:10.1242/jcs.200493

(Gladh et al., 2016), suggesting that its interaction with NRP1 and activation of PDGFRβ might be involved in spatial regulatory mechanisms in mural cells or between endothelial cells and adjacent pericytes. Many fundamental vascular processes depend on proper endothelial-to-pericyte communication, such as basement membrane formation, vascular stabilization, maintenance and remodeling (Armulik et al., 2011; Geevarghese and Herman, 2014). The need for PDGF-B signaling through PDGFRβ in angiogenesis and vascular homeostasis is well established, as is the role of NRP1 (Andrae et al., 2008; Koch, 2012; Zachary, 2014). Here, we show in an *ex vivo* system sensitive for intercellular crosstalk, that PDGF-D induces a pericyte behavior different from PDGF-B. We thus provide a first clue that PDGF-D–PDGFRβ signaling can be involved in intercellular crosstalk between endothelial cells and pericytes through the formation of PDGFRβ and NRP1 complexes. Detailed investigation of the PDGFRβ–NRP1 interaction in *in vitro* co-culture systems confirmed that occurrence of PDGFRβ–NRP1 complexes was primarily in response to PDGF-D stimulation. These clusters of PDGFRβ and NRP1 were predominantly found in pericyte protrusions that are in contact with endothelial cells, which could hint towards a potential spatially restricted signaling hub for intercellular crosstalk downstream of PDGF-D. This idea is further strengthened by our previous observation showing that $NG2^+$ cells display a mispatterning phenotype in the adult heart of $Pdgfd^{-/-}$ mice (Gladh et al., 2016). Thus, PDGF-D–PDGFRβ signaling by recruitment of NRP1 may actively modulate endothelial-cell–pericyte communication in temporally and spatially restricted events. Recently, we could show that PDGF-D, but not PDGF-B, promotes neuroendocrine tumor growth by activation of a subpopulation of PDGFRβ-positive tumor cells (Cortez et al., 2016). NRP1 is a good candidate to be a co-receptor for PDGF-D-induced PDGFRβ-signaling in this context, a hypothesis that waits to be investigated.

Taken together, we demonstrate that PDGF-D directly binds to NRP1, thereby altering the cellular distribution and availability of NRP1 for other signaling pathways, or recruiting NRP1 as a co-receptor for PDGF-D–PDGFRβ signaling (summarized in Fig. 8). These novel findings are the basis for further investigations to understand the biology of PDGF-D as well as NRP1, which have implications for clinical conditions, such as cardiovascular disorders or cancer.

MATERIAL AND METHODS

Materials

Commercially available recombinant proteins, human PDGF-D (1159-SB), human PDGF-B (220-BB), human VEGF-A_{165} (293-VE) human VEGF-A_{189} (8147-VE), and mouse NRP1 (5994-N1) were purchased from R&D Systems (Minneapolis, MN). Recombinant human VEGF-A_{121} (100-20A), VEGF-A_{165} (100-20) and PDGF-B (100-14B) were purchased from Peprotech (Rocky Hill, NJ) Recombinant human full-length (FL-)PDGF-D (TP760442) was purchased from OriGene Technologies Inc. (Rockville, MD). Biotinylated heparin from porcine intestinal mucosa was purchased from Merck Millipore (Darmstadt, Germany). Heparin (unfractionated) was purchased from Sigma-Aldrich (Schnelldorf, Germany). Recombinant rat NRP1 deletion constructs (Gu et al., 2002) were transfected into PAE cells using Lipofectamine 2000 reagent (Thermo Fisher Scientific). After 48 h, cells were harvested and lysed in lysis buffer (see Immunoprecipitation) to prepare protein solutions. Commercially available primary antibodies are presented in Table S1, and were used according to manufacturers' instructions.

Alignment

For the alignment of protein sequences, the EMBL-EBI online portal (www.ebi.ac.uk/tools/msa/) for pairwise or multiple sequence alignments was utilized. The Clustal Omega operation was used to generate the sequence alignments. Sequences from mature human growth factor proteins, without signal sequence and post transcriptionally removed latent peptide sequences were used for the study.

Modeling of PDGF-D three-dimensional structure

The amino acid sequence of core PDGF-D was loaded into the online portal of Swiss model (https://swissmodel.expasy.org/interactive) to model PDGF-D structure using VEGF-B (PDB ID: 2c7wA) as template. Graphic representation was prepared using Swiss Pdbviewer software (http://spdbv.vital-it.ch/). For surface electrostatic potential visualization, the color indication was set to 0=red, 1=white and 2=blue.

Cell culture

Standard *in vitro* cell culture conditions were applied. In brief, immortalized human foreskin fibroblasts (BJ-hTERT; ATCC, CRL-4001) and porcine aortic endothelial cells (PAE) stably transfected with human PDGFRβ (PAE-Rβ) (Bergsten et al., 2001) were cultured using Dulbecco's modified Eagle's medium (DMEM) with F12 (Thermo Fischer Scientific Inc., Waltham, MA) supplemented with 10 U/ml penicillin, 10 µg/ml streptomycin and 10% fetal calf serum (FCS) (all three Thermo Fisher Scientific Inc.). African green monkey kidney fibroblasts (COS-1, ATCC, CRL-1650) were cultured using DMEM (Thermo Fischer Scientific Inc.) supplemented with 10 U/ml penicillin, 10 µg/ml streptomycin and 10% FCS. Human umbilical vein endothelial cells (HUVECs; PromoCell, Heidelberg, Germany) and human brain micro-vascular pericytes (HBVPs; ScienCell Research Laboratories, Carlsbad, CA) were cultured on cell culture plates coated with gelatin (1% w/v in PBS) (Sigma Aldrich) and in endothelial cell growth medium 2 (EGM2) (PromoCell) including growth supplements (2.5% FCS) and 10 U/ml penicillin, 10 µg/ml streptomycin.

siRNA treatment

BJ-hTERT cells were cultured as described above (see Cell culture). BJ-hTERT were transfected with control siRNAs (siCONTROL) or siRNA against PDGFRβ or NRP1 (siPDGFRβ or siNRP1, respectively) (all Santa Cruz Biotechnology Inc.) using Lipofectamine RNAiMAX (Thermo Fisher Scientific) according to the manufacturer's recommendations. Following overnight incubation with the respective siRNA, the cells were plated for the specific assays, and further processed as described in the Direct cell stimulation or Immunofluorescence analysis section.

Solid-state protein-binding assay

96-well microtiter plates were coated with 50 µl of PDGF-D or PDGF-B solution at increasing amounts (0.2–25 ng/well) in 100 mM sodium carbonate buffer (pH 9.5) (Sigma Aldrich) for 16 h at 4°C. Wells were washed and non-specific binding sites blocked with 3% BSA/TBS. Recombinant mouse NRP1 (1 µg/ml) or rat NRP1 deletion mutant proteins (Gu et al., 2002) were allowed to bind for 1 h at room temperature. To test the effects of heparin on the NRP1 binding to growth factors, 10 µg/ml heparin (Sigma Aldrich) was added simultaneously with soluble mouse NRP1 to one half of the growth factor-coated wells. Bound NRP1 was detected using goat anti-mouse and rat NRP1 antibody (cat. no. AF566) or rabbit anti-NRP1 (clone no. EPR3113, cat. no. ab81321), and the corresponding horseradish peroxidase (HRP)-tagged secondary antibody (GE Healthcare, Uppsala, Sweden) and immunopure TMB substrate kit (Thermo Fisher Scientific Inc.). For direct binding of biotinylated heparin to growth factors, microtiter plates were coated with 50 µl of growth factor proteins (25 ng/well) and blocked as described above. Biotinylated heparin was added to the wells and bound heparin was detected using streptavidin conjugated to HRP and a TMB substrate kit as described above. A plate reader (POLARstar Omega; BMG Labtec GmbH, Ortenberg, Germany) was used to measure absorbance at 450 nm.

PDGF-D mutant protein production

PDGF-D core protein cDNA (Ser^{250}–Arg^{370}) was amplified from vector plasmids (Ponten et al., 2005) using specific primers to introduce single base mutations in the C-terminal region. The common forward primer 5′-TAGGATCCTCATACCATGATCGGAAG-3′ together with three different

Journal of Cell Science (2017) 130, 1365-1378 doi:10.1242/jcs.200493

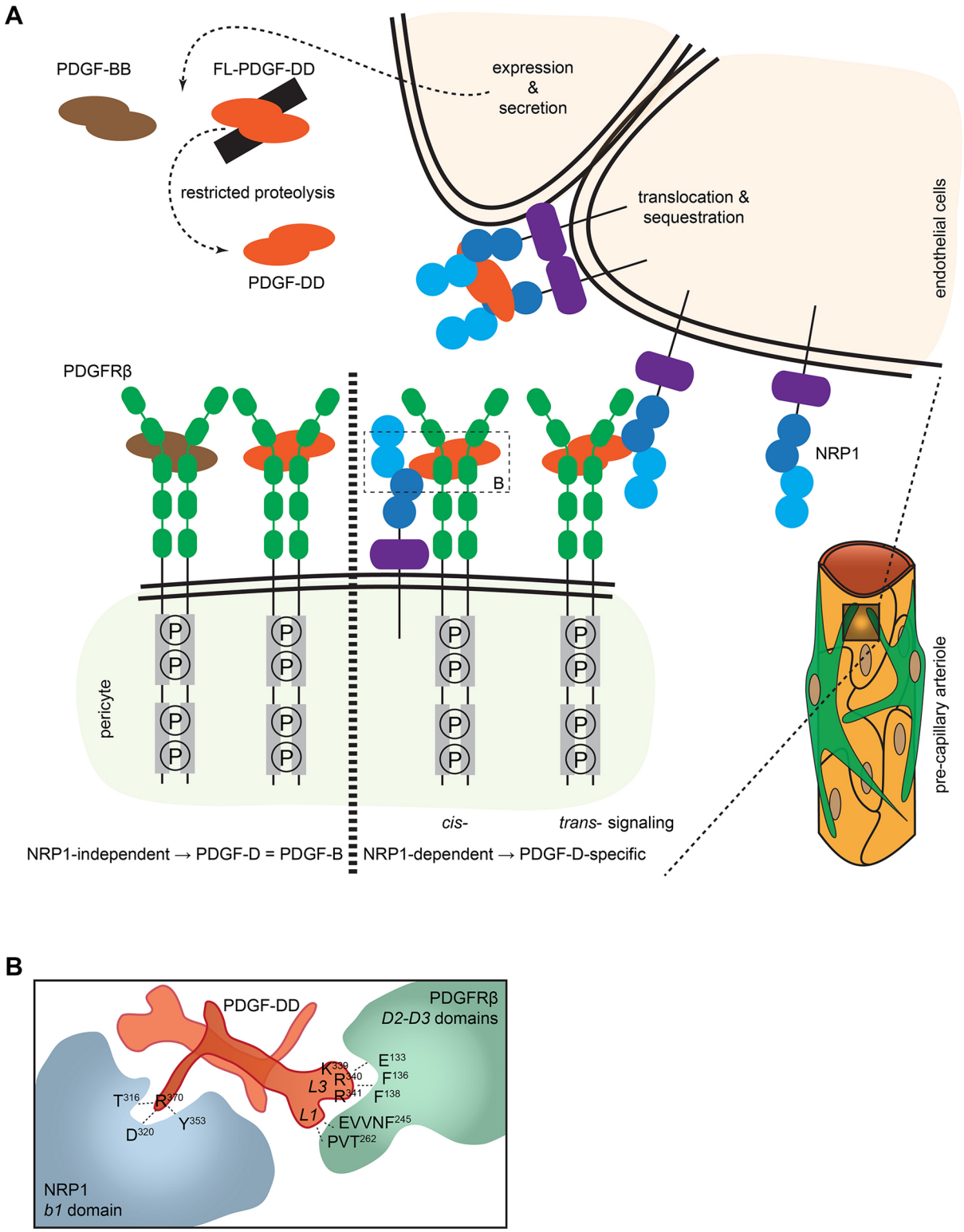

Fig. 8. Proposed model-of-action for PDGF-D-induced PDGFRβ–NRP1 complex formation, resulting in PDGF-D-specific receptor engagement and downstream signaling. (A) Overview of PDGF-D interaction with NRP1 and PDGFRβ in *cis* as well as in *trans*, between two adjacent cell types, here endothelial cells and pericytes. (B) Schematic illustration of the suggested simultaneous binding of the PDGF-DD dimer to NRP1 (b1-domain, left) and PDGFRβ (D2-D3 domains, right), with the potentially interacting amino acids indicated for NRP1 (Parker et al., 2012) or PDGFRβ (Shim et al., 2010). L1 and L3 mark loop I and loop III regions in PDGF-D, respectively.

reverse primers to amplify PDGF-D cDNA containing the wild type (wt) sequence 5′-TAGAATTCTTATCGAGGTGGTCTTGAGC-3′, PDGF-D with a truncated C-terminal Arg^{370} (-R) sequence 5′-TAGAATTCTTATC-AAGGTGGTCTTGAGCT-3′ and PDGF-D with a substitution of the C-terminal arginine to glycine (R→G) 5′-TAGAATTCTTATCCAGGT-GGTCTTGAGC-3′ were used for construct amplification. The amplified

Journal of Cell Science (2017) 130, 1365-1378 doi:10.1242/jcs.200493

constructs were cut and ligated into a modified pSecTag vector, using BamHI and EcoRI restriction enzymes, FastAP and T4 ligase (all Thermo Fisher Scientific Inc.). Ligated plasmid vectors were transformed into TOP10 *E. coli*, and amplified and purified with the respective preparation kits (Macherey-Nagel, Dueren, Germany) according to the manufacturer's recommendations. Plasmids containing the PDGF-D constructs were sent for sequencing using Sanger sequencing (GATC Biotech AG, Constance, Germany). Obtained sequences were visualized using 4Peaks software (by A. Griekspoor and Tom Groothuis, nucleobytes.com/4peaks/) and analyzed by using Sequence analysis software (www.informagen.com/SA/) for the correct base sequence. PDGF-D mutant protein constructs were transfected into PAE cells stably transfected with human PDGFRβ (PAE-Rβ) (Bergsten et al., 2001) or COS-1 cells. Cell lysates were prepared by direct addition of SDS sample buffer (63 mM Tris-HCl pH 6.8, 10% glycerol and 2% SDS). Conditioned medium was collected for direct application, or concentrated using 30 kDa cut-off concentrating columns (Merck Chemical and Life Sciences AB, Solna, Sweden).

Ligand blot

Recombinant human PDGF-D (R&D Systems) or concentrated supernatant from COS-1 cells overexpressing recombinant PDGF-D proteins were separated on a 10% SDS-PAGE gel and transferred onto a nitrocellulose membrane (both Thermo Fisher Scientific Inc.). After blocking of non-specific binding sites with 3% BSA/TBS-T the membrane was incubated with recombinant mouse NRP1 solution (1 µg/ml). Bound NRP1 was detected by incubation with goat anti-mouse and -rat antibody (cat. no. AF566) followed by the corresponding HRP-tagged secondary antibody. As loading control, PDGF-D proteins were detected by sequential incubation with goat anti-PDGF-D antibody (cat. no. AF1159) followed by corresponding HRP-tagged secondary antibody, and development was performed as described below (Direct cell stimulation).

Direct cell stimulation

BJ-hTERT cells were cultured in 24-well cell culture plates, serum-deprived for 4–6 h in DMEM/F12 with 0.2% FCS prior to stimulation with PDGF-D or PDGF-B. Cells were stimulated for 10 to 120 min at 37°C. Thereafter, cells were washed once with PBS and directly lysed in SDS sample buffer. Proteins were separated on a 4–12% SDS-PAGE gradient gel, transferred to nitrocellulose membranes and detected by sequential incubation with primary antibodies and corresponding HRP-tagged secondary antibodies according to the manufacturer's recommendations. For repeated detection of different proteins, the membranes were washed with stripping buffers (1: 200 mM glycine, 0.1% Tween 20, pH 2.8; and 2: 200 mM glycine, 500 mM NaCl, 0.1 % Tween 20 pH 9.6; Sigma Aldrich) and re-probed with new primary and secondary antibodies. Signals were detected by using an ECLprime reagent kit (GE Healthcare) and pictures were taken with the imaging system FluoroChem Q (Alpha Innotec GmbH, Kasendorf, Germany) and graphically handled using Image J software. All images were appropriately adjusted in brightness and contrast and processed with 'despeckle' noise reduction and 'smoothen' operations.

Immunofluorescence analysis

BJ-hTERT cells were cultured on gelatin-coated glass coverslips in six-well cell culture plates, and serum deprived for 4–6 h in DMEM/F12 with 0.2% FCS prior to stimulation with PDGF-D or PDGF-B (each 20 ng/ml). Cells were stimulated for 20 min at 37°C, thereafter medium was removed and cells fixed with ice-cold 4% paraformaldehyde (PFA) in PBS for 10 min at room temperature. Likewise, HUVECs and HBVPs were cultured alone or together on gelatin-coated glass coverslips in six-well cell culture plates, serum deprived for 4–6 h in EGM2 with 0.5% FCS and stimulated as described above. After fixation with 4% PFA in PBS cells were blocked with blocking buffer [serum-free protein blocking solution (DAKO, Glastrop Denmark)], supplemented with 0.2% Triton X-100 (Sigma-Aldrich) for >1 h at room temperature. Thereafter, cells were sequentially incubated with primary antibodies and corresponding fluorescently tagged secondary antibodies (Molecular Probes, Eugene, OR) in blocking buffer, according to the manufacturer's recommendations. Cells were mounted with ProLong Gold mounting medium containing 4,6-diamidino-2-phenylindole (DAPI; Molecular Probes). Evaluation of the staining and image capture of immunofluorescence micrographs was carried out by using an upright laser scanning, confocal microscope (LSM 700; Carl Zeiss GmbH, Göttingen, Germany).

Immunoprecipitation

Cells were cultured as described above. After serum deprivation, cells were stimulated with PDGF-D or PDGF-B (each 25 ng/ml) for 5 min at 37°C, transferred to 4°C and stimulation continued for 1 h. Cells were washed with PBS, and cross linker (DTSSP; Thermo Fisher Scientific Inc.) was added at a concentration of 2 mM for 2 h at 4°C. Excess cross linker was blocked by washing with 100 mM glycine in PBS (Sigma-Aldrich) for 15 min at 4°C. Thereafter, cells were lysed with lysis buffer (50 mM Tris-HCl pH 7.5, 150 mM NaCl, 1% Ipegal CA-630 and 1% Triton X-100), supplemented with PhosSTOP phosphatase inhibitor and Complete protease inhibitor cocktail (both Roche Diagnostics, Indianapolis, IN) for 1 h at 4°C, scraped and unresolved cell-debris was pelleted by centrifugation for 10 min at 15,000 ***g***. For immunoprecipitation, goat anti-human NRP1 antibody (C19) was pre-bound to protein-G–Sepharose (GE Healthcare, Uppsala, Sweden) at a concentration of 2 µg/sample, for >30 min at 4°C. Antibody-bound Sepharose was then added to cell lysates and incubated with end-over-end rotation for 16 h at 4°C. Thereafter, the Sepharose beads were washed with TBS, then the bound proteins were denatured in β-mercaptoethanol (Sigma Aldrich) containing SDS sample buffer, and SDS-PAGE was performed according to manufacturer's recommendations, and the proteins were detected by western blotting as described above (Direct cell stimulation).

Animals, *ex vivo* sprouting angiogenesis assays and live-imaging

Mice expressing membrane-bound GFP (Tg(CAG-GFP*)Hadj/J (CAG: GFP-GPI) (Rhee et al., 2006) and mice expressing dsRED under the control of the *Cspg4* (gene of NG2) promoter NG2DsRedBAC tg (Zhu et al., 2008) were cross bred to generate double-positive reporter mice (hereafter GFP–GPI/NG2DsRed). All mice had always ad libitum access to water and chow. All mouse strains were housed in accordance with local guidelines and regulations for animal research (Swedish Animal Welfare Board, Stockholm, Sweden). For the sprouting assay using embryo explants, embryos at embryonic day (E)13.5 were isolated and the limbs, head and lower body were removed. The upper body was cut into 1 mm^3 pieces and embedded between two layers of rat-tail collagen type I (Thermo Fischer Scientific Inc.) and cultivated in DMEM supplemented with 10 U/ml penicillin, 10 µg/ml streptomycin and 10% FCS (all three Thermo Fisher Scientific Inc.) including 30 ng/ml VEGF-A_{165} (Peprotech). For specific growth factor stimulation, the medium was changed to DMEM with 2.5% FCS and 30 ng/ml VEGF-A, 30 ng/ml PDGF-D (R&D Systems) or 30 ng/ml PDGF-B (Peprotech). After live imaging, samples were fixed with 4% PFA in PBS. For aortic ring sprouting assay, mice were killed between 4 to 6 weeks of age and thoracic aortas were isolated, cleaned from connective tissue, cut into 1 mm rings, embedded and cultivated as described above. For specific growth factor stimulation, the medium was changed to DMEM with 10% FCS and 30 ng/ml VEGF-A, 10 µg/ml control IgG (BioLegend, San Diego, CA), 30 ng/ml PDGF-D (R&D Systems) or 30 ng/ml PDGF-B (Peprotech).

For the embryo explant culture assay, 13 *z*-slices were acquired at each position every 23 min using an inverted laser-scanning confocal microscope (SP8, Leica Microsystems GmbH, Wetzlar, Germany), with a 10× (NA 0.3, air) objective and maintained at 37°C and 5% CO_2 with a humidifier system. For the aortic ring culture assay, 75 *z*-slices were acquired at each position every 20 min using the same microscope set-up with a 20× (NA 0.75, water immersion) objective.

Live-imaging quantification

Vessel sprouting speed was measured as the vessel elongation divided by time. Pericyte coverage was measured as the number of pericytes divided by vessel length at the start and the end frame of live imaging. The changes in pericyte coverage were plotted as percentages. Pericyte migration speed was calculated by tracking of individual pericytes ($NG2^+$ cells) over the period of live imaging. Pericytes with a defined distance to the endothelial sprout were considered as detached.

Statistical analysis

All presented experiments have been performed at least twice, except for embryo explant or aortic ring sprouting assays, which each have been performed once. Results from one representative experiment or the mean± s.d. of the replicate experiments are shown as indicated in the respective figure legend. Specific *P*-values and statistical tests used are indicated in the respective figure legend. A *P*-value<0.05 was considered as statistically significant.

Acknowledgements

The authors would like to thank Associate Professor Chenghua Gu (Harvard Medical School, MA, USA), and Alessandro Mega and Professor Arne Östman (Karolinska Institutet, Stockholm, Sweden) for their generous gifts of crucial reagents. The authors also like to thank Dr Yi Jin (Karolinska Institutet, Stockholm, Sweden) for his excellent technical assistance on time-lapse imaging and Zacharias Iredahl for his technical assistance.

Competing interests

The authors declare no competing or financial interests.

Author contributions

L.M. designed the study, performed experiments and drafted the manuscript. E.B.F. and H.G. performed experiments and drafted the manuscript. Y.W. and C.M. performed experiments. E.B.F., L.J. and U.E. assisted in the study design. All authors commented on the manuscript.

Funding

This study was supported by Vetenskapsrådet (Swedish Research Council; to L.J., U.E.), the Hjärt-Lungfonden (Swedish Heart and Lung Foundation; to U.E.), Cancerfonden (Swedish Cancer Society; to L.J., U.E.) and Karolinska Institutet (L.J., U.E.). L.M. was supported by the Svenska Sällskapet för Medicinsk Forskning (Swedish Society for Medical Research). C.M. was supported by a European Molecular Biology Organization (EMBO) fellowship, co-financed by Marie-Curie actions.

Supplementary information

Supplementary information available online at
http://jcs.biologists.org/lookup/doi/10.1242/jcs.200493.supplemental

References

Andrae, J., Gallini, R. and Betsholtz, C. (2008). Role of platelet-derived growth factors in physiology and medicine. *Genes Dev.* **22**, 1276-1312.

Andrae, J., Ehrencrona, H., Gallini, R., Lal, M., Ding, H. and Betsholtz, C. (2013). Analysis of mice lacking the heparin-binding splice isoform of platelet-derived growth factor A. *Mol. Cell. Biol.* **33**, 4030-4040.

Armulik, A., Genové, G. and Betsholtz, C. (2011). Pericytes: developmental, physiological, and pathological perspectives, problems, and promises. *Dev. Cell* **21**, 193-215.

Aspalter, I. M., Gordon, E., Dubrac, A., Ragab, A., Narloch, J., Vizán, P., Geudens, I., Collins, R. T., Franco, C. A., Abrahams, C. L. et al. (2015). Alk1 and Alk5 inhibition by Nrp1 controls vascular sprouting downstream of Notch. *Nat. Commun.* **6**, 7264.

Ball, S. G., Bayley, C., Shuttleworth, C. A. and Kielty, C. M. (2010). Neuropilin-1 regulates platelet-derived growth factor receptor signalling in mesenchymal stem cells. *Biochem. J.* **427**, 29-40.

Ballmer-Hofer, K., Andersson, A. E., Ratcliffe, L. E. and Berger, P. (2011). Neuropilin-1 promotes VEGFR-2 trafficking through Rab11 vesicles thereby specifying signal output. *Blood* **118**, 816-826.

Banerjee, S., Sengupta, K., Dhar, K., Mehta, S., D'amore, P. A., Dhar, G. and Banerjee, S. K. (2006). Breast cancer cells secreted platelet-derived growth factor-induced motility of vascular smooth muscle cells is mediated through neuropilin-1. *Mol. Carcinog.* **45**, 871-880.

Bergsten, E., Uutela, M., Li, X., Pietras, K., Östman, A., Heldin, C.-H., Alitalo, K. and Eriksson, U. (2001). PDGF-D is a specific, protease-activated ligand for the PDGF beta-receptor. *Nat. Cell Biol.* **3**, 512-516.

Borkham-Kamphorst, E., Meurer, S. K., Van de Leur, E., Haas, U., Tihaa, L. and Weiskirchen, R. (2015). PDGF-D signaling in portal myofibroblasts and hepatic stellate cells proves identical to PDGF-B via both PDGF receptor type alpha and beta. *Cell. Signal.* **27**, 1305-1314.

Cao, S., Yaqoob, U., Das, A., Shergill, U., Jagavelu, K., Huebert, R. C., Routray, C., Abdelmoneim, S., Vasdev, M., Leof, E. et al. (2010). Neuropilin-1 promotes cirrhosis of the rodent and human liver by enhancing PDGF/TGF-beta signaling in hepatic stellate cells. *J. Clin. Invest.* **120**, 2379-2394.

Cebe-Suarez, S., Grunewald, F. S., Jaussi, R., Li, X., Claesson-Welsh, L., Spillmann, D., Mercer, A. A., Prota, A. E. and Ballmer-Hofer, K. (2008). Orf virus VEGF-E NZ2 promotes paracellular NRP-1/VEGFR-2 coreceptor assembly via the peptide RPPR. *FASEB J.* **22**, 3078-3086.

Cortez, E., Gladh, H., Braun, S., Bocci, M., Cordero, E., Björkström, N. K., Miyazaki, H., Michael, I. P., Eriksson, U., Folestad, E. et al. (2016). Functional malignant cell heterogeneity in pancreatic neuroendocrine tumors revealed by targeting of PDGF-DD. *Proc. Natl. Acad. Sci. USA* **113**, E864-E873.

Delcombel, R., Janssen, L., Vassy, R., Gammons, M., Haddad, O., Richard, B., Letourneur, D., Bates, D., Hendricks, C., Waltenberger, J. et al. (2013). New prospects in the roles of the C-terminal domains of VEGF-A and their cooperation for ligand binding, cellular signaling and vessels formation. *Angiogenesis* **16**, 353-371.

Ehnman, M., Li, H., Fredriksson, L., Pietras, K. and Eriksson, U. (2009). The uPA/uPAR system regulates the bioavailability of PDGF-DD: implications for tumour growth. *Oncogene* **28**, 534-544.

Fantin, A., Herzog, B., Mahmoud, M., Yamaji, M., Plein, A., Denti, L., Ruhrberg, C. and Zachary, I. (2014). Neuropilin 1 (NRP1) hypomorphism combined with defective VEGF-A binding reveals novel roles for NRP1 in developmental and pathological angiogenesis. *Development* **141**, 556-562.

Fredriksson, L., Li, H. and Eriksson, U. (2004). The PDGF family: four gene products form five dimeric isoforms. *Cytokine Growth Factor. Rev.* **15**, 197-204.

Geevarghese, A. and Herman, I. M. (2014). Pericyte-endothelial crosstalk: implications and opportunities for advanced cellular therapies. *Transl. Res.* **163**, 296-306.

Gelfand, M. V., Hagan, N., Tata, A., Oh, W.-J., Lacoste, B., Kang, K.-T., Kopycinska, J., Bischoff, J., Wang, J.-H. and Gu, C. (2014). Neuropilin-1 functions as a VEGFR2 co-receptor to guide developmental angiogenesis independent of ligand binding. *Elife* **3**, e03720.

Gladh, H., Folestad, E. B., Muhl, L., Ehnman, M., Tannenberg, P., Lawrence, A.-L., Betsholtz, C. and Eriksson, U. (2016). Mice lacking platelet-derived growth factor d display a mild vascular phenotype. *PLoS ONE* **11**, e0152276.

Gu, C., Limberg, B. J., Whitaker, G. B., Perman, B., Leahy, D. J., Rosenbaum, J. S., Ginty, D. D. and Kolodkin, A. L. (2002). Characterization of neuropilin-1 structural features that confer binding to semaphorin 3A and vascular endothelial growth factor 165. *J. Biol. Chem.* **277**, 18069-18076.

Heldin, C. H. and Westermark, B. (1999). Mechanism of action and in vivo role of platelet-derived growth factor. *Physiol. Rev.* **79**, 1283-1316.

Hellberg, C., Schmees, C., Karlsson, S., Ahgren, A. and Heldin, C.-H. (2009). Activation of protein kinase C alpha is necessary for sorting the PDGF beta-receptor to Rab4a-dependent recycling. *Mol. Biol. Cell* **20**, 2856-2863.

Hsu, J. and Smith, J. D. (2012). Genome-wide studies of gene expression relevant to coronary artery disease. *Curr. Opin. Cardiol.* **27**, 210-213.

Huang, W. and Kim, H.-R. C. (2015). Dynamic regulation of platelet-derived growth factor D (PDGF-D) activity and extracellular spatial distribution by matriptase-mediated proteolysis. *J. Biol. Chem.* **290**, 9162-9170.

Karlsson, S., Kowanetz, K., Sandin, A., Persson, C., Ostman, A., Heldin, C.-H. and Hellberg, C. (2006). Loss of T-cell protein tyrosine phosphatase induces recycling of the platelet-derived growth factor (PDGF) beta-receptor but not the PDGF alpha-receptor. *Mol. Biol. Cell* **17**, 4846-4855.

Koch, S. (2012). Neuropilin signalling in angiogenesis. *Biochem. Soc. Trans.* **40**, 20-25.

Koch, S., van Meeteren, L. A., Morin, E., Testini, C., Weström, S., Björkelund, H., Le Jan, S., Adler, J., Berger, P. and Claesson-Welsh, L. (2014). NRP1 presented in trans to the endothelium arrests VEGFR2 endocytosis, preventing angiogenic signaling and tumor initiation. *Dev. Cell* **28**, 633-646.

Kofler, N. and Simons, M. (2016). The expanding role of neuropilin: regulation of transforming growth factor-beta and platelet-derived growth factor signaling in the vasculature. *Curr. Opin Hematol.* **23**, 260-267.

Lanahan, A. A., Hermans, K., Claes, F., Kerley-Hamilton, J. S., Zhuang, Z. W., Giordano, F. J., Carmeliet, P. and Simons, M. (2010). VEGF receptor 2 endocytic trafficking regulates arterial morphogenesis. *Dev. Cell* **18**, 713-724.

LaRochelle, W. J., Jeffers, M., McDonald, W. F., Chillakuru, R. A., Giese, N. A., Lokker, N. A., Sullivan, C., Boldog, F. L., Yang, M., Vernet, C. et al. (2001). PDGF-D, a new protease-activated growth factor. *Nat. Cell Biol.* **3**, 517-521.

Li, X., Ponten, A., Aase, K., Karlsson, L., Abramsson, A., Uutela, M., Backstrom, G., Hellstrom, M., Bostrom, H., Li, H. et al. (2000). PDGF-C is a new protease-activated ligand for the PDGF alpha-receptor. *Nat. Cell Biol.* **2**, 302-309.

Lindahl, P., Johansson, B. R., Leveen, P. and Betsholtz, C. (1997). Pericyte loss and microaneurysm formation in PDGF-B-deficient mice. *Science* **277**, 242-245.

Lindblom, P., Gerhardt, H., Liebner, S., Abramsson, A., Enge, M., Hellstrom, M., Backstrom, G., Fredriksson, S., Landegren, U., Nystrom, H. C. et al. (2003). Endothelial PDGF-B retention is required for proper investment of pericytes in the microvessel wall. *Genes Dev.* **17**, 1835-1840.

Mamluk, R., Gechtman, Z., Kutcher, M. E., Gasiunas, N., Gallagher, J. and Klagsbrun, M. (2002). Neuropilin-1 binds vascular endothelial growth factor 165, placenta growth factor-2, and heparin via its b1b2 domain. *J. Biol. Chem.* **277**, 24818-24825.

Parker, M. W., Xu, P., Li, X. and Vander Kooi, C. W. (2012). Structural basis for selective vascular endothelial growth factor-A (VEGF-A) binding to neuropilin-1. *J. Biol. Chem.* **287**, 11082-11089.

Pellet-Many, C., Frankel, P., Jia, H. and Zachary, I. (2008). Neuropilins: structure, function and role in disease. *Biochem. J.* **411**, 211-226.

Pellet-Many, C., Frankel, P., Evans, I. M., Herzog, B., Jünemann-Ramirez, M. and Zachary, I. C. (2011). Neuropilin-1 mediates PDGF stimulation of vascular smooth muscle cell migration and signalling via p130Cas. *Biochem. J.* **435**, 609-618.

Pellet-Many, C., Mehta, V., Fields, L., Mahmoud, M., Lowe, V., Evans, I., Ruivo, J. and Zachary, I. (2015). Neuropilins 1 and 2 mediate neointimal hyperplasia and re-endothelialization following arterial injury. *Cardiovasc. Res.* **108**, 288-298.

Plein, A., Fantin, A. and Ruhrberg, C. (2014). Neuropilin regulation of angiogenesis, arteriogenesis, and vascular permeability. *Microcirculation* **21**, 315-323.

Ponten, A., Folestad, E. B., Pietras, K. and Eriksson, U. (2005). Platelet-derived growth factor D induces cardiac fibrosis and proliferation of vascular smooth muscle cells in heart-specific transgenic mice. *Circ. Res.* **97**, 1036-1045.

Rhee, J. M., Pirity, M. K., Lackan, C. S., Long, J. Z., Kondoh, G., Takeda, J. and Hadjantonakis, A.-K. (2006). In vivo imaging and differential localization of lipid-modified GFP-variant fusions in embryonic stem cells and mice. *Genesis* **44**, 202-218.

Roth, L., Prahst, C., Ruckdeschel, T., Savant, S., Westrom, S., Fantin, A., Riedel, M., Heroult, M., Ruhrberg, C. and Augustin, H. G. (2016). Neuropilin-1 mediates vascular permeability independently of vascular endothelial growth factor receptor-2 activation. *Sci. Signal.* **9**, ra42.

Shim, A. H.-R., Liu, H., Focia, P. J., Chen, X., Lin, P. C. and He, X. (2010). Structures of a platelet-derived growth factor/propeptide complex and a platelet-derived growth factor/receptor complex. *Proc. Natl. Acad. Sci. USA* **107**, 11307-11312.

Ustach, C. V. and Kim, H.-R. C. (2005). Platelet-derived growth factor D is activated by urokinase plasminogen activator in prostate carcinoma cells. *Mol. Cell. Biol.* **25**, 6279-6288.

Ustach, C. V., Huang, W., Conley-Lacomb, M. K., Lin, C.-Y., Che, M., Abrams, J. and Kim, H.-R. C. (2010). A novel signaling axis of matriptase/PDGF-D/ss-PDGFR in human prostate cancer. *Cancer Res.* **70**, 9631-9640.

Wang, Z., Ahmad, A., Li, Y., Kong, D., Azmi, A. S., Banerjee, S. and Sarkar, F. H. (2010). Emerging roles of PDGF-D signaling pathway in tumor development and progression. *Biochim. Biophys. Acta* **1806**, 122-130.

Zachary, I. (2014). Neuropilins: role in signalling, angiogenesis and disease. *Chem. Immunol. Allergy* **99**, 37-70.

Zhu, X., Bergles, D. E. and Nishiyama, A. (2008). NG2 cells generate both oligodendrocytes and gray matter astrocytes. *Development* **135**, 145-157.